# Universal Form of Hall Coefficient in K and Rb Doped Single Crystal $C_{60}$

Li Lu,* Vincent H. Crespi, M. S. Fuhrer, A. Zettl, and Marvin L. Cohen
*Department of Physics, University of California at Berkeley, Berkeley, California 94720*
and
*Materials Sciences Division, Lawrence Berkeley Laboratory, Berkeley, California 94720*

(Received 9 June 1994)

We report the first Hall effect measurements on K and Rb doped single crystals of $C_{60}$. The temperature dependence of the Hall coefficient $R_H$ for each material and the variation in $R_H$ *between* the two materials can be accounted for solely by the variations in lattice constant, yielding a universal relationship of $R_H$ versus lattice constant for the alkali-doped $C_{60}$ systems. The results are interpreted in the context of a strongly disordered system in which the Hall coefficient is sensitive to disorder broadening at the Fermi energy.

PACS numbers: 72.15.Eb, 61.46.+w, 63.20.Kr

The alkali-doped $C_{60}$ superconductors [1] compose a family of uniquely tunable binary superconductors with high transition temperatures. Variations in lattice constant yield variations in $T_c$ over an order of magnitude from ~3 to ~30 K [2]. The electronic structure [3] and transport properties [4,5] of these materials are strongly affected by the orientational disorder of the $C_{60}$ constituents, raising questions as to the most appropriate picture for the electronic states. The Hall effect can provide information as to the nature of the relevant electronic structure. Unfortunately, the only existing Hall effect measurements were performed on a granular K doped $C_{60}$ film [6] with a nonmetallic resistivity and zero-dimensional fluctuation conductivity near $T_c$. Since Hall effect measurements are known to be sensitive to sample granularity [7], experiments on single crystal samples are necessary to obtain accurate information on electronic and transport processes.

We present the first measurements of the Hall effect on K and Rb doped single crystal $C_{60}$ samples. The temperature dependence of the Hall coefficients of $K_3C_{60}$ and $Rb_3C_{60}$ from the superconducting transition to room temperature can be described by a universal function of lattice constant. The results are interpreted within a conventional band picture with disorder broadening of electronic states near the Fermi level and a lattice-constant-dependent density of states. In this temperature range the Fermi surface is strongly modified by scattering on a length scale on the order of the interball distance.

Thin platelike $C_{60}$ single crystals of typical size $500 \times 200 \times 30\ \mu m^3$ with shiny facets were doped with K or Rb following standard techniques [8]. Prior to doping, eight gold wires were bonded to the edges of the crystal. The iterated dopes and anneals were guided by *in situ* monitoring of the two and four probe resistance. The Hall effect was determined by applying an external magnetic field of up to 8 T perpendicular to the largest crystal face and passing an ac current of ~10 mA at 37 Hz through the sample. A current balance technique [9] was used to zero the Hall voltage at zero magnetic field. Both positive and negative magnetic field sweeps were used throughout to eliminate low-frequency drift effects.

Figure 1 shows the temperature-dependent Hall coefficient $R_H$ from just above the superconducting transition to 300 K for optimally doped $K_3C_{60}$ and $Rb_3C_{60}$ samples. $R_H$ for $K_3C_{60}$ is negative and increases linearly with increasing temperature with a slope of $0.0055 \times 10^{-9}\ m^3/C\ K$. The room temperature value of $-1.4 \times 10^{-9}\ m^3/C$ coincides with the free electron value for three electrons per $C_{60}$. We emphasize, however, that a direct comparison with the free electron result is of limited utility in a system with a complex Fermi surface. The Hall coefficient for $Rb_3C_{60}$, also linearly temperature dependent with similar slope, is displaced upward from that of $K_3C_{60}$ and has a zero crossing at $T \sim 120$ K.

We characterize the possible effects of variations in effective sample geometry by sytematically measuring the doping dependence of $\rho$ and $R_H$. The functional form of $\rho(T)$ is doping independent, indicating that both the intrinsic residual resistivity and the intrinsic temperature-dependent resistivity are also doping independent [10]. Figure 2 shows the Hall mobility $\mu_H = R_H/\rho$ for three K doped samples which have room temperature resistivities in the ratio 1:2:3, a ratio consonant with substantial differences in doping between the samples. As shown in Fig. 2, $\mu_H$ is doping invariant, suggesting that the phase

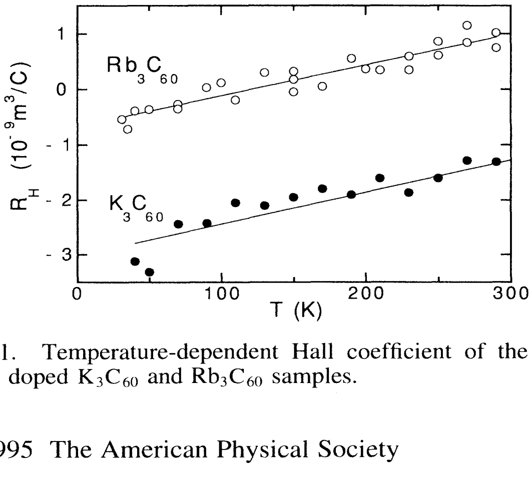

FIG. 1. Temperature-dependent Hall coefficient of the optimally doped $K_3C_{60}$ and $Rb_3C_{60}$ samples.

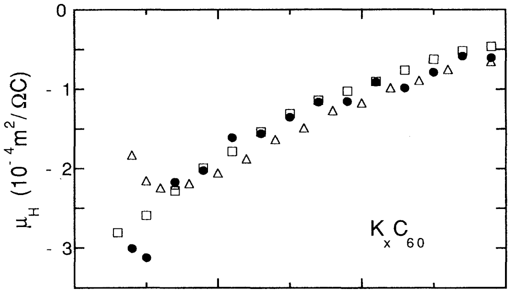

FIG. 2. Temperature dependence of the apparent Hall mobility of three $K_xC_{60}$ samples with different doping levels. The resistivity ratios at 300 K are △ : □ : ● = 3 : 2 : 1. Note that the $x$ in $K_xC_{60}$ is a sample average; the actual material will consist of a mixture of line phases with $x = 0, 1, 3, 4$, and/or 6.

boundaries inside of the thin-plate samples are parallel to the major faces, a geometry in which the functional forms of $\rho(T)$ and $R_H(T)$ are intrinsic to the $A_3C_{60}$ ($A$ = K, Rb) phase [11]. In addition, the ratio of extrapolated $T = 0$ resistivities for the optimally doped $Rb_3C_{60}$ and $K_3C_{60}$ samples was $[\rho(Rb_3C_{60})/\rho(K_3C_{60})] \approx 1.6$ [with $\rho(K_3C_{60}) = 1.0$ mΩ cm], a value consistent with the best estimates of the ratio of instrinsic resistivities for these two compounds [12–15] and indicative of similar effective geometries for our optimally doped samples.

Previous work demonstrates a strong influence of thermal expansion upon the form of $\rho(T)$ in $Rb_3C_{60}$ [16]. This result suggests that lattice thermal expansion should be taken into account in a discussion of $R_H(T)$. The lattice thermal expansion of $A_3C_{60}$ in the temperature range of interest can be adequately expressed as $a(T) = a_0 + bT$, where $b$ is $3.52 \times 10^{-4}$ Å$K^{-1}$ for $K_3C_{60}$ [17] and $4.40 \times 10^{-4}$ Å$K^{-1}$ for $Rb_3C_{60}$ [18]. Using these results, we plot $R_H$ as a function of lattice constant in Fig. 3. We obtain a striking relation—the difference in $R_H$ between $K_3C_{60}$ and $Rb_3C_{60}$ samples at a given temperature can be ascribed purely to the difference in the lattice constant between the two materials. This result suggests that the variation in $R_H$ with temperature for a given sample can also be attributed purely to changes in lattice constant. Apparently, *$R_H$ at constant volume is temperature independent for both materials.* A simple linear fit yields a lattice constant dependence of $R_H = [-2.8 + 13.9(a - 14.15)] \times 10^{-9}$ m$^3$/C, where $a$ is measured in angstroms.

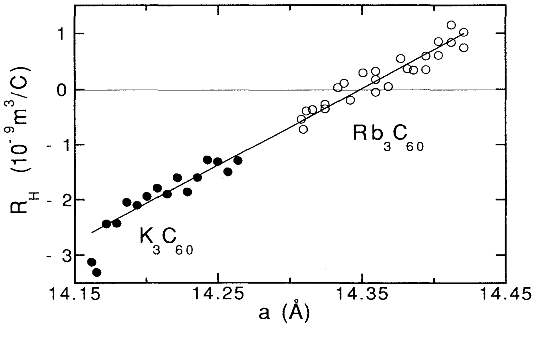

FIG. 3. Hall coefficient as a function of lattice constant for the optimally doped $K_3C_{60}$ and $Rb_3C_{60}$ samples.

Prior calculations of the Hall coefficient using the Jones-Zener solution [19] of the Boltzmann equation in an orientationally ordered system at zero temperature with isotropic scattering time yield $R_H = 7 \times 10^{-9}$ m$^3$/C for both $K_3C_{60}$ and $Rb_3C_{60}$ [20]. This result, which is weakly pressure dependent, arises from a complex weighted average of curvature over the Fermi surface. The result is at variance with the present experiments, wherein the Hall coefficient is much smaller in absolute magnitude and negative over a broad temperature range. In addition, the universal dependence of $R_H$ on lattice constant suggests a pressure dependence much stronger than that calculated. Since the Hall coefficient is sensitive to details of the Fermi surface curvature, it is plausible that the discrepancy between theory and experiment is due to disorder-induced modification of the Fermi surface which is not taken into account in the orientationally ordered calculation. Although other etiologies could be envisioned (nonadiabatic effects, electron-electron correlation), the primary electronic feature determining the character of the electronic states appears to be the strong orientational disorder.

The common source of a temperature-dependent Hall coefficient is a temperature-dependent anisotropy in the scattering time at temperatures below $\Theta_{\mathrm{Debye}}$. Judging from experimental and theoretical indications of moderate total electron-phonon coupling [21] and small electron-alkali-phonon coupling [22], the primary contribution to the electron-phonon scattering time can plausibly be attributed to high frequency on-ball optical phonons. The near Einstein nature of $C_{60}$ optical phonons and the strong electronic disorder suggest that any purely phonon anisotropy is weak and insensitive to temperature. Although the interball vibrational modes are expected to show significant dispersion, their frequencies are too low (~100 K) to explain the temperature dependence in $R_H$ observed up to 300 K. In addition, the measured universal dependence on lattice constant argues strongly (if somewhat circularly) against a significant temperature-dependent phonon contribution to $R_H$. Instead, we must seek an explanation invoking a mechanism which itself shows universal scaling. In particular, we examine the combined influence of orientational disorder and universal scaling of the density of states.

We begin our discussion of a model for the universal scaling of $R_H$ by introducing the appealing theoretical construct of the scattering length surface [23]. In this treatment, the Hall conductivity $\sigma_{xyz}$ of a two-dimensional system is identified with the number of flux quanta that thread a surface constructed by tracing the circuit of the vector scattering path length $\vec{\ell} = \vec{v}_k \tau_k$ as $\vec{k}$ circumscribes the Fermi surface (the three-dimensional case is treated as an integral over these two-dimensional constructs). The Hall coefficient $R_H$ is obtained from the ratio $R_H = \sigma_{xyz}/\sigma_{xx}\sigma_{yy}$. For a single-sheet Fermi surface with isotropic scattering, the resulting scattering path locus is simply a circle (sphere in 3D) which yields the free electron result of $R_H = -(1/nec)$. More complex Fermi surfaces with anisotropic scattering times yield additional loops in the scattering length locus which contribute in accord with the sign of circulation of the scattering length vector about these regions.

Calculations using a tight-binding disordered supercell, a cluster Bethe lattice, and a disorder-smeared virtual crystal [4] all yield a Fermi surface for the disordered system composed of pairs of parallel smeared sheets in the Cartesian directions with square electronlike regions centered at $\Gamma$, $X$, and $K$ (the region around $K$ is severely smeared). The electronlike nature of the disordered Fermi surface is consistent with the predominately negative Hall coefficient. We model the disorder by considering large supercells with the disorder incorporated into the unit cell. Since this model system has perfect order, the resulting Fermi surface is well defined and unsmeared, albeit quite complex due to the very large unit cell. Qualitatively, this Fermi surface will mimic the cluster Bethe result of a smeared quasi Fermi surface, but instead of true smearing the Fermi surface will have fine detail over a width consistent with the zero-temperature mean free path. This fine detail will consist of both numerous small electronlike and holelike pockets and the complex local curvature of the larger sections of Fermi surface, sections which may either encompass the $\Gamma$ and $X$ points or bridge across the zones.

The numerous small holelike and electronlike pockets will contribute oppositely to the integral determining $R_H$, presumably yielding a small net contribution to the Hall coefficient. Anisotropy in the scattering length along the large-scale sections of the Fermi surface will lead to the formation of secondary loops associated with negative-curvature regions of these extended portions of the Fermi surface. Since regions of negative curvature are generally closer in $k$ space to the bottom of the band than are regions of positive curvature, these negative curvature regions should have larger Fermi velocities (the bands must disperse more strongly to reach the Fermi surface over a smaller distance in $k$ space). As shown in Fig. 4, the secondary loops then contribute opposite in sign from the main loop contribution [23]. The variation in $R_H$ with lattice constant can be qualitatively modeled by assuming that the relative $k$-space extent of the disorder broadening of the Fermi surface increases with increasing lattice constant: As the $k$-space extent of the disorder increases, the secondary loops grow and the Hall coefficient increases.

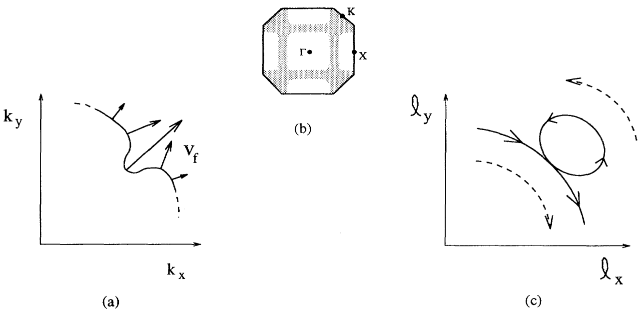

FIG. 4. (a) Blowup of the disordered Fermi surface, showing variation in $v_f$ near a region of negative curvature (a "dip"). The Fermi velocity is larger toward the origin which is the center of a large electronlike region. (b) Large-scale view of Fermi surface. Shading delineates region containing the complex disordered Fermi surface. Adapted from [4]. (c) Circuit traced by scattering length vector $\vec{l} = \tau \vec{v}_f$ corresponding to the portion of Fermi surface shown in (a). The circulation in the secondary loop is opposite to that in the primary loop. A similar argument applies to "bumps" in the Fermi surface.

The question remains how an increase in lattice constant could yield an increase in the disorder broadening at the Fermi level. If the effects of the disorder have a characteristic energy scale which is to lowest order independent of the lattice constant, then the $k$-space extent of the disorder broadening will be an increasing function of density of states at the Fermi level and hence an increasing function of lattice constant. The increased residual resistivity of $Rb_3C_{60}$ compared to $K_3C_{60}$ [12–15] provides some support for this scenario. The universal scaling of $R_H$ is then a natural consequence of the universal scaling of the density of states as a function of the lattice constant [24]. At low disorder broadening the Hall conductivity is dominated by the primary loop in $\ell$ space which is produced by the large regions of enclosed electrons. At large disorder broadening the Hall conductivity is dominated by secondary loops in $\ell$ space which contribute to $R_H$ opposite in sign to the primary loop. This argument suggests that the Hall coefficient $R_H$ in $A_3C_{60}$ will increase from negative values at low disorder broadening ($K_3C_{60}$ sample at low $T$ and small density of states) to positive values at larger disorder broadening ($Rb_3C_{60}$ sample at high $T$ and large density of states). The behavior is similar to that suggested [25] for disordered nearly free electron metals, wherein the Hall coefficient is inversely dependent on the density of states.

A quantitative calculation requires knowledge of the total area of the secondary loops. The extent of the loops in the radial direction is easily estimated from the variation in Fermi velocity across the smearing region. More difficult to estimate is the filling factor of the secondary loops within these annular regions. Within a simple model [26] one obtains

$$\sigma_{xyz} = \sigma_{xyz}^0 (1 - \gamma C) . \tag{1}$$

The prefactor $\sigma_{xyz}^0$ is the (unknown) Hall conductivity at infinitesimal disorder, expected to be of the order of the free electron value. $C$ is a geometrical factor of order unity associated with the filling factor of the secondary loops. The parameter $\gamma$ is the ratio of the energy scale of the disorder to the Fermi energy. Alternatively, it can be expressed as $\gamma \sim (1/\ell k_f)$, $\ell$ the disorder-induced mean free path and $k_f$ the characteristic Fermi wave vector. The Hall coefficients for $K_3C_{60}$ and $Rb_3C_{60}$ extrapolated linearly to $T = 0$ can be combined with estimates of the $T = 0$ disorder-induced mean free paths from upper critical field data [14,15] to determine the geometric factor $C$. We obtain $C \sim 1.9$, of the correct sign and order of magnitude.

Although finite phonon energies, thermal smearing, and true (nonsupercell) disorder will wash out the finest structure of the disordered supercell Fermi surface, the functional form of $R_H$ is primarily determined by the Fermi surface sampling of the large-scale variation in $v_f$, a large-scale feature which should not be washed out by moderate smearing. Temperature-dependent thermal smearing will contribute a nonuniversal term to the volume dependence of the Hall coefficient. However, taking a mean free path of 12 Å for $Rb_3C_{60}$ at $T = 0$ [15] and $v_f = 1.5 \times 10^8$ cm/sec [15], a simple estimate for the energy scale of the disorder yields $\Delta E \approx (\hbar v_f/\ell) \approx$ 1400 K, substantially larger than the temperature range of this experiment—temperature-dependent thermal smearing should make a minor nonuniversal contribution to $R_H$. We also note that the orientational disorder in alkali-doped $C_{60}$ appears to be frozen in the temperature regime of this experiment, arguing against the possibility of nonuniversal contributions to $R_H$ from temperature dependence in the nature of the orientational disorder.

Hall effect measurements on $K_3C_{60}$ and $Rb_3C_{60}$ single crystal samples yield $R_H$ as a universal function of lattice constant, apparently regardless of whether dilation is caused by thermal expansion or steric effects. A qualitative model incorporating lattice-constant-dependent disorder broadening at the Fermi level is consistent with this universal form and accounts for the discrepancy between the experimental results and previous calculations on orientationally ordered systems. The theoretical treatment yields a simple prediction for the pressure dependence of the Hall coefficient, namely, the same universal functional dependence on volume should be evinced if the volume change is induced by pressure rather than temperature or species of alkali atom. A similar argument applies to alloys such as $Rb_xCs_{3-x}C_{60}$ or $K_xRb_{3-x}C_{60}$, materials which would be expected to have temperature-dependent Hall coefficients in accord with this universal form.

This work was supported by National Science Foundation Grants No. DMR-90-17254 (L.L., M.F., and A.Z.) and No. DMR-9120269 (V.H.C. and M.L.C.), and the Director, Office of Energy Research, Office of Basic Energy Sciences, Materials Sciences Division of the U.S. Department of Energy under Contract No. DE-AC03-76SF00098.

---

*Permanent address: Institute of Physics, Chinese Academy of Sciences, Beijing 100080, China.

[1] A. F. Hebard *et al.*,Nature (London) **350**, 600 (1991).
[2] O. Zhou *et al.*, Science **255**, 833 (1992).
[3] E. L. Shirley and S. G. Louie, Phys. Rev. Lett. **71**, 133 (1993); M. P. Gelfand and L. P. Lu, Phys. Rev. Lett. **68**, 1050 (1992).
[4] E. J. Mele and S. C. Erwin (unpublished).
[5] J. P. Lu and M. Gelfand, Phys. Rev. B **46**, 4367 (1992).
[6] T. T. M. Palstra, R. C. Haddon, A. F. Hebard, and J. Zaanen, Phys. Rev. Lett. **68**, 1054 (1992).
[7] Barrier regions and/or hopping conduction between grains will modify the Hall coefficient. N. F. Mott and E. A. Davis, *Electronic Processes in Non-Crystalline Materials* (Clarendon Press, Oxford, 1971), pp. 53–55; *ibid.* (Clarendon Press, Oxford, 1979), 2nd ed., pp. 56 and 92.
[8] X.-D. Xiang *et al.*, Science **256**, 1190 (1992).
[9] R. H. Friend and N. Bett, J. Phys. E **13**, 294 (1980).
[10] A. Zettl *et al.*, J. Superconductivity **7**, 639 (1994).
[11] Assuming a filling fraction of $\beta$ for the $A_3C_{60}$ phase relative to an insulating background material, a parallel-plate geometry yields $R_H \propto \beta$ and $\rho \propto \beta$ such that $\mu_H = R_H/\rho$ is independent of $\beta$ as observed, whereas a percolative island model yields $R_H \propto \beta$ and $\rho \propto \beta^n$ ($n \geq 2$) such that $\mu_H \propto \beta^{n-1}$, at variance with the experimental results.
[12] A. F. Hebard, T. T. M. Palstra, R. C. Haddon, and R. M. Fleming, Phys. Rev. B **48**, 9945 (1993).
[13] X.-D. Xiang *et al.*, Nature (London) **361**, 54 (1993).
[14] J. G. Hou *et al.*, Solid State Commun. **86**, 643 (1993).
[15] J. G. Hou *et al.*, Physica (Amsterdam) **228C**, 175 (1994).
[16] W. A. Vareka and A. Zettl, Phys. Rev. Lett. **72**, 4121 (1994).
[17] Q. Zhu and J. E. Fisher (private communication).
[18] O. Zhou *et al.*, *Novel Forms of Carbon,* edited by C. L. Renschler, J. J. Pouch, and D. M. Cox (Materials Research Society, San Francisco, CA, 1992), Vol. 270, p. 191.
[19] H. Jones and C. Zener, Proc. R. Soc. London A **145** (1934).
[20] S. C. Erwin and W. E. Pickett, Phys. Rev. B **46**, 14 257 (1992).
[21] M. Schluter, M. Lannoo, M. Needles, and G. A. Baraff, Phys. Rev. Lett. **68**, 526 (1992); C. M. Varma, J. Zaanen, and K. Raghavachari, Science **245**, 989 (1991); V. H. Crespi *et al.*, Phys. Rev. B **46**, 12 064 (1992); L. Degiorgi *et al.*, Phys. Rev. B **49**, 7012 (1994).
[22] B. Burk, V. H. Crespi, A. Zettl, and M. L. Cohen, Phys. Rev. Lett. **72**, 3706 (1994).
[23] N. P. Ong, Phys. Rev. B **43**, 193 (1991).
[24] A. Oshiyama and S. Saito, Solid State Commun. **82**, 41 (1992).
[25] J. M. Ziman, Adv. Phys. **13**, 578 (1967).
[26] V. H. Crespi, L. Lu, and M. L. Cohen (unpublished).